Micromechanical Switch-Based Zero-Power Chemical Detectors for Plant Health Monitoring

Sila Deniz Calisgan, Vageeswar Rajaram, Sungho Kang, Antea Risso, Zhenyun Qian, *Member, IEEE*, and Matteo Rinaldi, *Senior Member, IEEE*

***Abstract*— In this paper, for the first time we demonstrate zero-power volatile-organic-chemical (VOC) detectors based on micromechanical switches suitable for plant health monitoring. Differently from state-of-the-art active chemical sensors, the device presented here exploits a completely passive, chemically-sensitive switch based on a bimaterial microcantilever and a passive switch-based readout mechanism to detect VOCs exceeding a pre-determined concentration released by unhealthy plants. When exposed to target VOCs, the polymer/metal bimaterial beam bends downward and trigger the switch due to the stress induced from the absorption of chemicals in the polymer layer. Here we show experimental demonstrations of detecting toluene, hexenol (cis-3-Hexen-1-ol, a chemical released from plants under attack by pests) and ethanol, respectively, with our fabricated prototypes. The demonstrated high sensitivity to ethanol (∼ *8 nm/ppm*) and hexenol (∼ *3.3 nm/ppm*) was achieved by the optimization of device geometries showing a great promise of the proposed technology to ultimately achieve *10s* ppm detection limit (with a sub-micron contact gap and voltage bias) which is required for the device operation in close proximity to a plant in an open environment. [2020-0190]**

***Index Terms*— Cantilever, chemical detection, gas sensor, micromechanical, microswitch, plant defense, polymer, volatile organic chemical, zero-power.**

I. Introduction

EARLY and accurate detection of pest and disease outbreaks in crop fields is critical for minimizing losses and maximizing production yield especially in low-income countries. Conventional methods of plant health monitoring often rely on manual inspection and decision-making which are only effective after the plant is visibly affected by the pest or disease. Advanced imaging tools (e.g. hyperspectral cameras [1]) with sophisticated sensor fusion have been demonstrated for accurate early-stage detection of outbreaks. However, such an approach is unfeasible for smallholder farming and only applies to specific agriculture sectors with high return-on-investment rate (e.g. vineyards) in developed countries due to the high deployment and maintenance cost of the required sensor systems.

Studies show that crops with green leaves release a significant amount of VOCs (e.g. hexenals, hexenols, hexyl acetates, toluene) when attacked by pests or diseases [2]–[4]. The released VOCs play a role in the plants' defense system and their amount depends on the severity of the damage [2], [5], [6]. The localized concentration can go up to ∼10 parts per million (ppm) when a leaf is damaged in multiple spots [6]. Thus, detecting these VOCs can be an effective way to identify and subsequently respond to attacks by pest and diseases. State-of-the-art VOC sensors based on photoionization detectors (PIDs) [7] are expensive and unsuited for remote deployment in the crop fields because of their high power consumption. On the other hand, microelectromechanical systems (MEMS) based solutions can potentially reduce the system cost and enable the deployment of chemical sensor networks with high granularity in remote locations. The state-of-the-art polymer-coated MEMS cantilever based detectors have been demonstrated for such applications (e.g. electronic nose) in static and dynamic measurement modes [8], [9]. The static mode measures the bending displacement in the cantilever with optical or resistive outputs [10], [11]. On the other hand, dynamic mode utilizes the frequency shift due to the mass loading in the devices [12], [13]. Both types require active readout circuitry which consumes constant electrical power at standby (i.e. in the absence of targeted VOCs). The continuous power consumption significantly limits their battery lifetime and increases the battery replacement and maintenance costs, effectively limiting their scalability for large-scale deployment.

Recently, the need for active electronic sensors for screening the environment has been challenged with the development of passive OFF-but-alert sensors [14], [15]. These "event-driven" sensors exploit the energy present in the signal of interest itself to perform the detection.

Our group has previously demonstrated the device concept using a chemically-actuated polymer/metal micromechanical switch for zero-power ethanol sensing in a conference [16]. In this paper we show an improved design with over 20× increased sensitivity and the detection of relatively low concentrations (∼1237 ppm and ∼ 3220 ppm) of green leaf

Manuscript received May 15, 2020; accepted June 7, 2020. Date of publication July 17, 2020; date of current version October 7, 2020. This work was supported by the Grand Challenges Explorations initiative from Bill and Melinda Gates Foundation. Subject Editor R. Ghodssi. *(Corresponding authors: Sila Deniz Calisgan; Matteo Rinaldi.)*

Sila Deniz Calisgan, Vageeswar Rajaram, Sungho Kang, and Antea Risso are with the Northeastern SMART Center, Northeastern University, Boston, MA 02115 USA (e-mail: calisgan.s@northeastern.edu; rajaram.v@northeastern.edu; kang.su@northeastern.edu; risso.a@northeastern.edu).

Zhenyun Qian is with the Department of Electrical and Computer Engineering, Northeastern University, Boston, MA 02115 USA (e-mail: z.qian@northeastern.edu).

Matteo Rinaldi is with the Northeastern SMART Center, Northeastern University, Boston, MA 02115 USA (e-mail: m.rinaldi@northeastern.edu).

Color versions of one or more of the figures in this article are available online at http://ieeexplore.ieee.org.

Digital Object Identifier 10.1109/JMEMS.2020.3007309

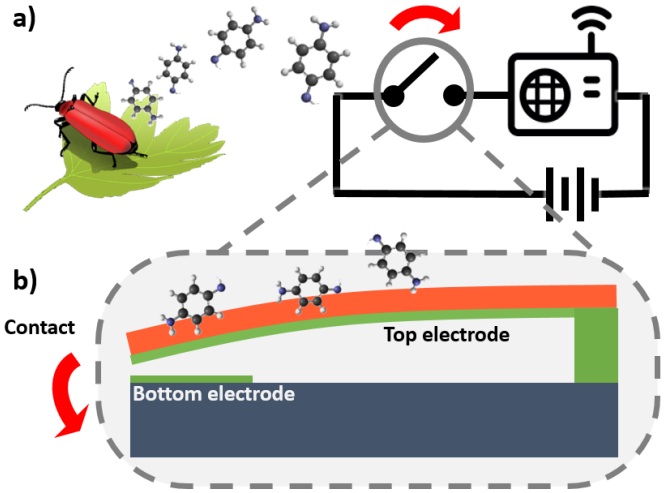

Fig. 1. a) Circuit schematic of the switch based zero-power chemical sensor connecting to a battery and a radio transmitter for the wireless detection of VOCs released by damaged plants. The switch turns ON only when an above-threshold chemical concentration is detected triggering the radio transmitter. b) Schematic of a bimaterial cantilever-based switch actuated by the interaction with VOCs.

VOCs (i.e. hexenol and toluene vapor). The experimental results demonstrate a great potential of the proposed device for zero-power plant health monitoring in a large-area crop field (Fig. 1a).

II. Design

The core element of the proposed zero-power VOC detector is a bimaterial micro-cantilever that comprises a metal and polymer layer. When the cantilever is exposed to specific kinds of VOC vapor, the polymer chains interact with the VOC molecules which are smaller compared to chains. These interactions between VOCs and polymer chains are similar to solvent-polymer interactions that is governed by the Flory-Huggins theory for nonideal mixing:

$$\ln(a) = \ln(1-\varphi\chi) + \left(1+\frac{1}{N}\right)\varphi + \chi\varphi^2 \qquad (1)$$

where a is the relative vapor pressure of the solvent, N is the fraction of molar volume of the polymer to the solvent, φ is the segment molar fraction of the polymer and χ is composition dependent Flory-Huggins interaction parameter [17], [18] which can be used to find compatible polymer-solvent pairs. In our case with polymer film and solvent vapor, the composition variable $\varphi \sim 1$ due to the high polymer volume fraction.

The top layer of bimaterial beam (i.e. polymer layer) is chosen to absorb targeted chemicals (i.e swelling effect) whereas the bottom layer (metal layer) is insensitive. The stress created by this swelling in the polymer layer is used as the actuation mechanism. Whereas the polymer expands in volume due to the swelling, the underlaying metal remains unaffected, causing the bimaterial beam to bend down (Fig. 1b). When the swelling reaches a threshold (i.e., the VOC concentration absorbed exceeds a specific value), the top and bottom electrodes touch each other, thereby completing an electrical path across the switch which then can be used to trigger a next stage electronics (e.g. turn ON a radio transmitter). The physical contact gap prevents any subthreshold leakage currents leading to a zero standby power consumption, which is a key enabler for extended battery lifetime.

A. Material Optimization

In order to make an effective and highly sensitive sensor, the volumetric expansion of polymer layer should be maximized in response to specific VOC molecules of interest. In other words, its affinity (how strongly the polymer interacts with the VOC compared to its intramolecular monomer-monomer interactions) to the targeted VOC molecules needs to be as high as possible (higher the affinity, the greater is the volumetric expansion). Thus, the polymer should be chosen such that compared to other polymers, it has large affinity towards specific VOCs that are typically released by plants.

In this study, we chose gold (Au) as first layer for the bimaterial stack due to its high conductivity and low residual stress in the material. The analytes cis-3-Hexen-1-ol (referred to as hexenol from here on) and toluene was chosen as the primary chemicals of interest, since they are the common indicators showing that the plant is under stress due to pest or diseases [2], [5], [9]. Poly(methyl methacrylate) (PMMA) was chosen as the functional polymer layer due to its affinity to toluene and ease of fabrication [18]. In addition, we also studied ethanol since it is a chemical that is relatively safe to be used in the lab environment with our test setup. The ethanol response of the devices was used to establish a fair comparison of sensitivity between the previous work and this paper.

For the targeted VOCs and the polymer layer the mass uptake was a physical absorption mechanism instead of chemical bonding. In physical absorption the absorbed molecules could diffuse back from the polymer surface (solvent desorption) when the VOCs were not present in the environment (i.e. the plant was no longer emitting VOCs). Therefore, this physical absorption was preferred for reversible switch operations and reusable detectors.

B. Polymer Thickness and Device Dimensions

The effect of polymer thickness over the device sensitivity was simulated to determine the optimum thickness of PMMA for a given Au thickness (Fig. 2). The thermal expansion model in COMSOL is used to mimic the volumetric expansion of the polymer in the steady state condition [19]. A heat source was applied to the bimaterial cantilever where the thermal expansion coefficient of Au was set to be 0 since this layer is inactive and does not experience any expansion upon chemical exposure. It was assumed in this model that the entire thickness of the PMMA layer contributes to the expansion since the all the PMMA is expected to interact with targeted VOC over a time period (typically 10s mins for the selected thickness). The sensitivity scales with the square of the length of the cantilever. This relation can be utilized to set the threshold of the devices lithographically based on the plant and the different targeted VOC levels.

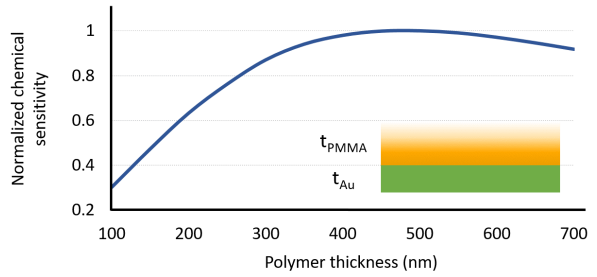

Fig. 2. Simulation of the normalized chemical sensitivity of the bimaterial beam as a function of PMMA thickness for a fixed Au thickness t_{Au} = 250 nm. The sensitivity (defined as tip displacement/gas concentration) reaches maximum for a PMMA thickness around 500 nm.

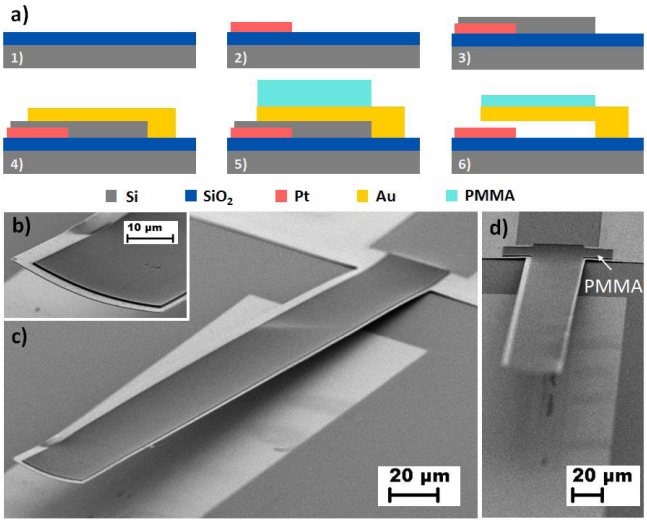

Fig. 3. a) 4-mask microfabrication process of the proposed zero-power chemical detectors. b) The scanning electron microscope (SEM) image of the tip region of the cantilever. c) and d) SEM images of the fabricated devices with different anchor designs altering the side PMMA coverage.

C. Device Fabrication

The device fabrication process (Fig. 3a) started with single side polished wafer coated with 500 nm of silicon dioxide (SiO_2) via low pressure chemical vapor deposition (LPCVD). This oxide layer serves as a separation from the bulk silicon therefore it is not patterned. The bottom contact, 10 nm of titanium (Ti) (for adhesion) and 40 nm of platinum (Pt) were then deposited using electron beam evaporation and patterned with liftoff. The photolithography was assisted with lift off resist (LOR) to eliminate the sidewalls around the Pt layer. A sacrificial layer of 600 nm of silicon was deposited thereafter with sputtering deposition to set the gap between top and bottom contacts. Then top contact electrode, 10 nm of Ti and 250 nm of gold (Au), was deposited with electron beam evaporation and patterned with liftoff. The gold layer also serves as bottom metal layer in the bimaterial beam. The top layer of the cantilever was formed by spin-coating PMMA with an initial thickness of 1.4 μm then thinning to 550 nm or100 nm using oxygen plasma in order to achieve a more controllable thickness and bending after release. The devices with different thickness of PMMA were designed to study the

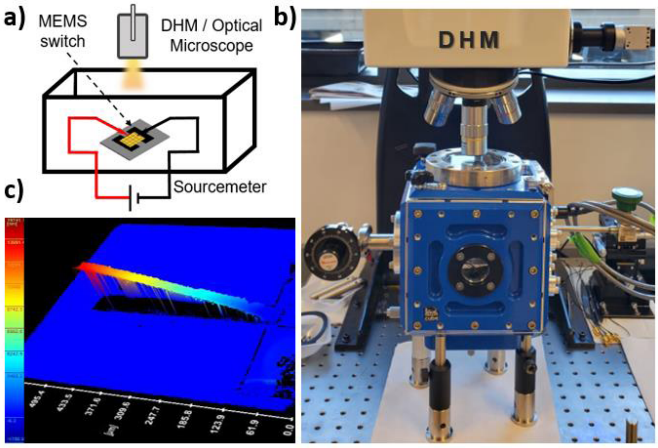

Fig. 4. a) Schematic of the experimental setup with sealed chamber (3.54 L inner volume) for testing. A sourcemeter is used as a voltage source and simultaneously measures the current flowing through the switch. b) Experimental setup of the chemical chamber placed under a DHM microscope. c) The 3D profile of a bimaterial cantilever measured with the DHM. The cantilever shown here (40 μm in width and 300 μm in length) has a measured contact gap of 15.2±0.2 μm in the tip region of the bimaterial beam.

effect on the sensitivity and beam curvature. The last step of fabrication is the release in which the sacrificial amorphous silicon layer was isotropically etched with xenon difluoride (XeF_2). Scanning electron microscope (SEM) images after release are shown in Fig. 3c and 3d.

Other than the PMMA thickness, the devices were also designed to have different length (300 nm and 400 nm), width (20 nm and 40 nm) and anchor types. In particular, two anchor types (Type A and B - inset images in Fig. 5) were designed to study the effect of the side polymer coverage on the beam profile. To determine which design provides the least residual stress induced curvature in the profile, the released devices were investigated with digital hologram microscopy (DHM) which constructs 3D profiles of the imaged surface (Fig. 4c). The initial beam profiles (before testing with any chemicals) of Type B devices with side PMMA extensions show 25-30% larger gap compared to Type A with same beam dimensions (Fig. 5). Similar to the lateral curving (along width) of the cantilever due to residual stress seen in Fig. 3b, we expect the side-extensions of Type B devices to also contribute extra curvature. Therefore, the anchor point of these designs create a "bowl-shape", increasing the take-off angle of the cantilever, and resulting in a larger contact gap (which results in a higher threshold). Thus, to achieve smaller detection thresholds in gas concentration, the Type A designs are employed for the VOC detectors.

III. Experimental Setup and Results

A. Test Setup

The fabricated devices were tested in a sealed chamber (Fig. 4a and 4b) filled with air (treated as an ideal gas) and toluene, hexenol or ethanol vapors were generated by evaporating a fixed volume of these liquids (99.8% toluene, 98% cis-3-Hexen-1-ol and 99% ethanol) which were purchased from

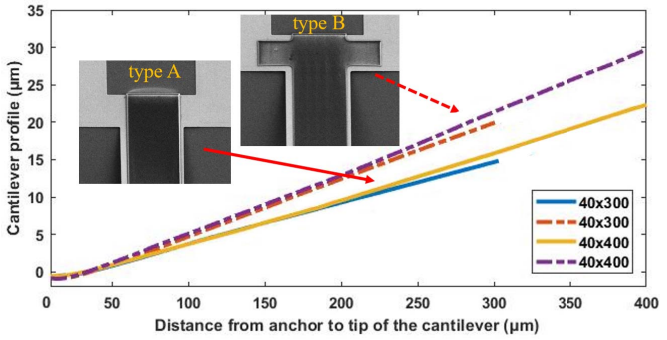

Fig. 5. Measured cantilever profiles of the devices with different lengths and anchor types. Dashed lines and solid lines show the profiles of devices with type B and type A anchors, respectively. Inset: Top view SEM images of the anchor regions.

Sigma Aldrich and used directly without dilution. The toluene and ethanol concentration in the chamber were calculated from the initial amount of liquid and the general gas law (when the drop was completely vaporized):

$$n_{VOC} = \frac{\rho_{VOC} * V_{VOC}}{MW_{VOC}} \tag{2}$$

$$n_{total} = \frac{P * V}{R * T} \tag{3}$$

$$C_{VOC} = \frac{n_{VOC}}{n_{total}} \tag{4}$$

where, n_{VOC} is the amount of chemical in moles (Eq. 2), V_{VOC} is the initial liquid volume (50 μL for toluene and 75 μL for ethanol) dropped into the chamber with micropipettes, ρ_{VOC} is the density and MW_{VOC} is molecular weight of chemicals. Equation 3 is used to estimate the total amount of gas molecules (n_{total}) in the chamber where P is the chamber pressure, V is the chamber volume (3.54 L), R is the Boltzmann gas constant and T is the temperature (22.85 °C) [11]. The ethanol was observed to fully evaporate 60 min after the chamber is closed (Fig. 6a). C_{VOC} is the concentration of the VOC vapor in the overall chamber (Eq. 3).

In the case of hexenol, the liquid phase reached equilibrium with its vapor phase before the liquid drop was fully evaporated. Therefore, the time to reach final concentration needs to be evaluated in addition to the final saturation vapor concentration. The steady state hexenol concentration was calculated to be 1237 ppm based on the ratio between its saturation vapor pressure (0.94 mmHg) and the atmospheric pressure. The time required to reach final vapor concentration was estimated from the ratio of relative evaporation rates between ethanol and hexenol. The evaporation rate of hexenol was not readily available in literature, therefore the value for hexanol (lacking C = C bond) was used with the assumption that the C = C bond in hexenol doesn't change the physical properties significantly compared to hexanol [20]. The relative evaporation rate based on n-butyl acetate (BuAc = 1) for ethanol is 1.7 and 0.05 for hexanol which was the value used for hexenol here. Based on these relative rates and surface area of the liquids (liquid hexenol surface area was doubled compared to ethanol experiment to decrease the

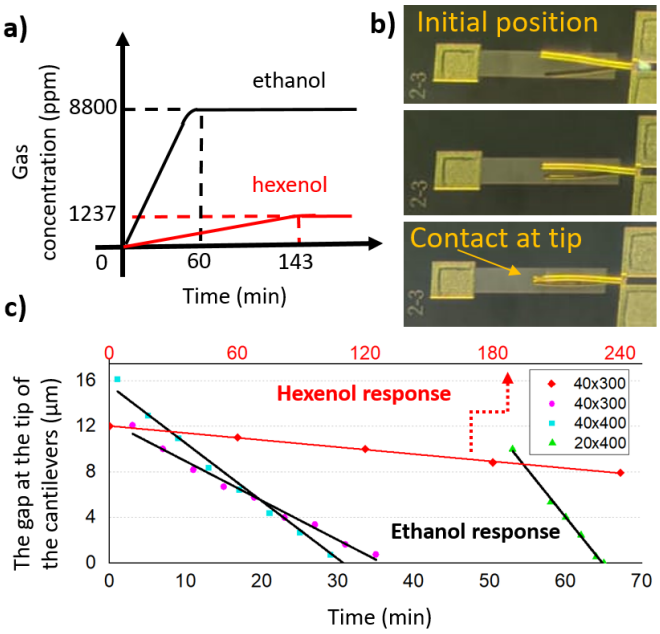

Fig. 6. a) Calculated vapor concentration as a function of time. Final ethanol concentration is 8800 ppm after 60 min. Final hexenol concentration of 1237 ppm is reached after 143 min. b) Optical microscope images of a cantilever in 3 statuses of bending. c) The position of cantilever tip vs. time in response to ethanol or hexenol vapor. The legend shows the dimensions (width and length in μm) of the cantilevers where the thickness of PMMA (550 nm) and Au (250 nm) is same for all of them. Note that the time axes start after the equilibrium is reached (constant concentration for both analytes).

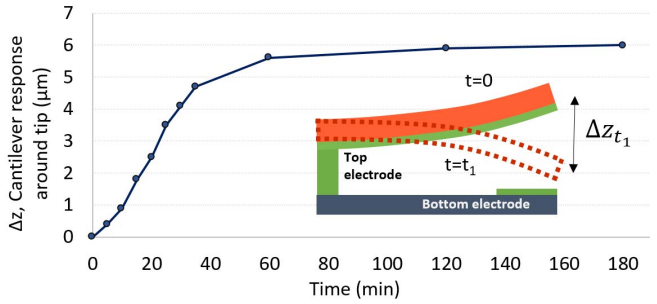

Fig. 7. The response of a device with 100-nm PMMA to toluene vapor. Δz_{t_1} represents the change in the gap around tip region at t_1. Toluene was fully evaporated with a final concentration of 3220 ppm which results in a gap reduction of 6 μm. Note that the time was counted after the equilibrium is reached.

experiment time), it was determined that hexenol reached a saturation concentration of 1237 ppm after 143 min (Fig 7a).

The testing chamber was kept in an environment with unchanged humidity throughout the experiments. By doing so, the water vapor absorbed by the PMMA layer could only affect the initial cantilever profile. The cantilevers didn't show any humidity-induced drift in their profile for more than 10 hours in a closed testing chamber after the initial DHM calibration and prior to the experiments.

B. Results

The DHM was used to monitor the profile of the cantilevers continuously and measure the displacement of their contact

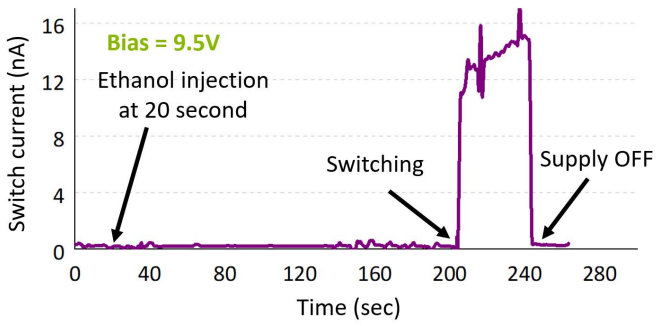

Fig. 8. The Measured current of a device in response to ethanol while a 9.5 V bias voltage is being applied.

tips over time after the VOC concentration reaches saturation (Fig. 6c). Magnified images of the cantilever were taken through a microscope to show the change of beam profile as the interaction with the chemicals progresses (Fig. 6b). It was discovered that narrower devices exhibit higher sensitivity than wider ones. While the sensitivity improvement due to optimized PMMA thickness is expected from the simulation, we suspect that the correlation between the sensitivity and the beam width is associated with the residual stress that caused the beam to wrap transversally (Fig. 3b). We observed a larger transversal bending in wider beams which is expected to reduce the tip displacement (i.e. longitudinal bending) when the beams are exposed to chemicals due to the effectively increased beam stiffness.

The response (i.e. tip displacement) of a device (300 μm in length and 40 μm in width) with a PMMA thickness of 100 nm was recorded over time, after toluene was added into the chamber (Fig. 7). The sensitivity was measured to be 1.86 nm/ppm which results in 3.28× (the response ratio of 550 nm-thick and 100 nm-thick PMMA) less sensitive devices as shown in Fig. 2. It is expected that a sensitivity of 6.1 nm/ppm for toluene can be achieved with an increased PMMA thickness of 500 nm. The device response shows the saturation (maximum bending with corresponding chemical concentration) was reached 60 min after the liquid injection to the media (Fig. 7).

The devices with 550 nm-thick PMMA were tested with ethanol and hexenol vapors. The 40 × 300 device (width × length in μm) showed a tip displacement of 4090 nm in response to a hexenol vapor with a concentration of 1237 ppm (∼3.3 nm/ppm). Based on the ethanol sensitivity of different designs, a hexenol sensitivity as high as ∼7.8 nm/ppm is expected to be achieved with the 20 × 400 design. The result shows that longer and narrower cantilevers are more sensitive and also faster in response. Compared to the previous demonstration [16], in this work, a 20× higher sensitivity was enabled by a 3× thicker PMMA layer (increased chemical absorption) and a 3× narrower cantilever (increased out-of-plane displacement in response to VOC absorption).

C. Electrical Response

To demonstrate the ON/OFF function of these switches, the switch with a 550 nm PMMA thickness (dimensions of 40 μm in width and 300 μm in length) was tested in a smaller enclosed chamber (∼150 mL) with ethanol as the triggering VOC and the current flow through it continuously monitored by a sourcemeter. In this experiment, a bias voltage was applied between the top and bottom contacts of the switch to reduce the gap and facilitate the closing of the gap by leveraging the electrostatic force and pull-in effect [21]. It is worth noting that, the applied voltage does not result in a standby power consumption thanks to the zero leakage current. The pull-in voltage of the device was measured to be 11.5 V. Based on that, the bias voltage was selected to be 9.5 V ensuring a high stability when not exposed to the chemicals. (The switch was monitored with a 9.5 V bias voltage for more than 30 minutes without any chemical input to verify the voltage bias doesn't result in false positive detection.) The switch was triggered by ethanol with a concentration of 1100 ppm (in the 150 mL chamber) resulting in a sensitivity of 8.2 nm/ppm (Fig. 8). Note that, the device shown here is not the representative of the best device in terms of contact cleanliness. The devices with a clean contact (from same fabrication batch) show the ON resistance of 135 Ω, which is suitable for connecting to a next-stage electrical load (e.g. transmitter, detector) to activate more functions [22].

IV. Conclusion

The device presented here exploits a zero-power switch-based read-out mechanism to detect above-threshold VOC concentrations. The physical gap between the contacts enabled zero standby power consumption for the next generation large-scale crop field monitoring. PMMA/Au bimaterial cantilevers were used for the detection of three different VOCs leveraging the swelling effect in the polymer layer upon absorption of the chemicals. Compared to the previous work, the new devices with the optimized geometries in this work showed an improved threshold to ethanol of 1100 ppm and a sensitivity of 8.2 nm/ppm. Likewise, the lowest threshold was found to be ∼1237 ppm (sensitivity ∼3.3 nm/ppm) for hexenol. The sensitivity to toluene was demonstrated to be 1.8nm/ppm which indicates that a higher sensitivity of 6.1 nm/ppm can be achieved upon optimization of the PMMA thickness. Future work will be focused on compensating for residual stress to minimize the contact gap which will allow for lower thresholds. Employing folded beam designs with a contact gap ∼500 nm [14] is expected to bring down the threshold to ∼ 60 ppm, with a further possible improvement via the voltage-based threshold scaling [21].

Acknowledgment

The authors thank Prof. Marilyn Minus, Dr. Wenjun Zhang, and Xuanhang Wu for valuable discussions and the staff of the George G. Kostas Nanoscale Technology and Manufacturing Research Center at Northeastern University where the devices were fabricated. This work was funded by the Grand Challenges Explorations (GCE) initiative from Bill and Melinda Gates Foundation.

REFERENCES

[1] O. M. Grant, H. Ochagavía, J. Baluja, M. P. Diago, and J. Tardáguila, "Thermal imaging to detect spatial and temporal variation in the water status of grapevine (Vitis vinifera L.)," *J. Horticultural Sci. Biotechnol.*, vol. 91, no. 1, pp. 43–54, Jan. 2016.

[2] A. Kessler, "Defensive function of herbivore-induced plant volatile emissions in nature," *Science*, vol. 291, no. 5511, pp. 2141–2144, Mar. 2001.

[3] A. C. Heiden, K. Kobel, M. Komenda, R. Koppmann, M. Shao, and J. Wildt, "Toluene emissions from plants," *Geophys. Res. Lett.*, vol. 26, no. 9, pp. 1283–1286, May 1999.

[4] M. Kallenbach, Y. Oh, E. J. Eilers, D. Veit, I. T. Baldwin, and M. C. Schuman, "A robust, simple, high-throughput technique for time-resolved plant volatile analysis in field experiments," *Plant J.*, vol. 78, no. 6, pp. 1060–1072, Jun. 2014.

[5] J. Wei and L. Kang, "Roles of (Z)-3-hexenol in plant-insect interactions," *Plant Signaling Behav.*, vol. 6, no. 3, pp. 369–371, Mar. 2011.

[6] R. Fall, T. Karl, A. Hansel, A. Jordan, and W. Lindinger, "Volatile organic compounds emitted after leaf wounding: On-line analysis by proton-transfer-reaction mass spectrometry," *J. Geophys. Res., Atmos.*, vol. 104, no. D13, pp. 15963–15974, Jul. 1999.

[7] H. Zhu *et al.*, "Flow-through microfluidic photoionization detectors for rapid and highly sensitive vapor detection," *Lab Chip*, vol. 15, no. 14, pp. 3021–3029, 2015.

[8] M. K. Baller *et al.*, "A cantilever array-based artificial nose," *Ultramicroscopy*, vol. 82, nos. 1–4, pp. 1–9, Feb. 2000.

[9] J. Laothawornkitkul *et al.*, "Discrimination of plant volatile signatures by an electronic nose: A potential technology for plant pest and disease monitoring," *Environ. Sci. Technol.*, vol. 42, no. 22, pp. 8433–8439, Nov. 2008.

[10] A. Boisen and T. Thomas, "Design & fabrication of cantilever array biosensors," *Mater. Today*, vol. 12, no. 9, pp. 32–38, 2009.

[11] C. Steffens, F. L. Leite, A. Manzoli, R. D. Sandoval, O. Fatibello, and P. S. P. Herrmann, "Microcantilever sensors coated with a sensitive polyaniline layer for detecting volatile organic compounds," *J. Nanosci. Nanotechnol.*, vol. 14, no. 9, pp. 6718–6722, Sep. 2014.

[12] D. Then, A. Vidic, and C. Ziegler, "A highly sensitive self-oscillating cantilever array for the quantitative and qualitative analysis of organic vapor mixtures," *Sens. Actuators B, Chem.*, vol. 117, no. 1, pp. 1–9, Sep. 2006.

[13] Y. Dong, W. Gao, Q. Zhou, Y. Zheng, and Z. You, "Characterization of the gas sensors based on polymer-coated resonant microcantilevers for the detection of volatile organic compounds," *Anal. Chim. Acta*, vol. 671, nos. 1–2, pp. 85–91, Jun. 2010.

[14] Z. Qian, S. Kang, V. Rajaram, C. Cassella, N. E. McGruer, and M. Rinaldi, "Zero-power infrared digitizers based on plasmonically enhanced micromechanical photoswitches," *Nature Nanotechnol.*, vol. 12, no. 10, pp. 969–973, Oct. 2017.

[15] S. H. Khan *et al.*, "Ultra-low-power chemical sensor node," in *Proc. GOMAC Tech*, 2018, pp. 1–4.

[16] S. D. Calisgan, V. Rajaram, Z. Qian, S. Kang, A. Risso, and M. Rinaldi, "Zero-power chemical sensor based on a polymer/metal micromechanical switch," in *Proc. IEEE SENSORS*, Oct. 2019, pp. 1–4.

[17] S. Enders and B. A. Wolf, Eds., *Polymer Thermodynamics: Liquid Polymer-Containing Mixtures*, vol. 238. Springer, 2011.

[18] M. Vayer, A. Vital, and C. Sinturel, "New insights into polymer-solvent affinity in thin films," *Eur. Polym. J.*, vol. 93, pp. 132–139, Aug. 2017.

[19] A. Singh and M. Mukherjee, "Swelling dynamics of ultrathin polymer films," *Macromolecules*, vol. 36, no. 23, pp. 8728–8731, Nov. 2003.

[20] C. A. Ward and G. Fang, "Expression for predicting liquid evaporation flux: Statistical rate theory approach," *Phys. Rev. E, Stat. Phys. Plasmas Fluids Relat. Interdiscip. Top.*, vol. 59, no. 1, p. 429, 1999.

[21] V. Rajaram, Z. Qian, S. Kang, N. E. McGruer, and M. Rinaldi, "Threshold scaling of near-zero power micromechanical photoswitches using bias voltage," in *Proc. IEEE SENSORS*, Oct. 2017, pp. 1–3.

[22] S. D. Calisgan, S. Kang, V. Rajaram, Z. Qian, and M. Rinaldi, "Threshold-triggered MEMS-CMOS infrared resonant detector with near-zero standby power consumption," in *Proc. 20th Int. Conf. Solid-State Sens., Actuators Microsyst. Eurosensors XXXIII (TRANSDUCERS EUROSENSORS XXXIII)*, Jun. 2019, pp. 637–640.

Sila Deniz Calisgan received the B.Sc. degree in electrical and electronics engineering from Middle East Technical University (METU), Ankara, Turkey, in 2017. She is currently pursuing the Ph.D. degree in materials, devices, and systems in electrical and computer engineering with Northeastern University, Boston, MA, USA. She previously worked in mobile millirobots during her internship with the Max Plank Institute for Intelligent Systems, Stuttgart, Germany. Her research focuses on polymer-based chemical sensing for plant health monitoring, zero power IR MEMS sensors with AlN resonant sensors for chemical and IR sensing.

Vageeswar Rajaram received the B.Tech. degree in electronics and instrumentation engineering from the Amrita School of Engineering, Coimbatore, India, in 2012, and the M.S. degree in electrical and computer engineering from Northeastern University, Boston, MA, USA, in 2015, where he is currently pursuing the Ph.D. degree in electrical engineering. His research interests primarily include micro/nano electromechanical systems (MEMS/NEMS) devices, low/zero power infrared (IR) sensors, AlN resonant sensors (chemical, IR), and optical MEMS.

Sungho Kang received the B.S. degree in electrical engineering from the University of Illinois at Urbana–Champaign, Champaign, IL, USA, in 2014, and the M.S. degree in electrical and computer engineering from Northeastern University, Boston, MA, USA, in 2017, where he is currently pursuing the Ph.D. degree in electrical engineering. His research focuses on low/zero power IR MEMS sensors, plasmonic metamaterials for application in chemical and IR sensing, and AlN resonant sensors.

Antea Risso was born in Cuneo, Italy, in 1992. She received the dual B.S. degree in telecommunication engineering from the Polytechnic University of Turin, Italy, and Tongji University, China, in 2014, the triple M.S. degree in nanotechnology from the Polytechnic University of Turin, the Institut National Polytechnique of Grenoble, France, and the Ecole Polytechnique Feìdeìrale of Lausanne, Switzerland, in 2016. She is currently pursuing the Ph.D. degree in nanotechnology with Northeastern University. She gathered research experience during her internships with the IBM Almaden Research Center, San Jose, CA, USA, and the Khademhosseini Laboratory (affiliated to the Harvard-MIT and Brigham and Women's Hospital), Boston, MA, USA. From 2016 to 2018, she was a Sales Executive with Arduino (Switzerland and USA). Finally, before joining Northeastern University, she interned as a Marketing Manager with Ilum China-Photovoltaic Industrial roofs in Shanghai, China. During her Ph.D., She is currently Researcher in the field of nano/micro electro-mechanical-systems (N/MEMS), Her focus is to develop an infrared-based sensor to help optimize water usage in agriculture.

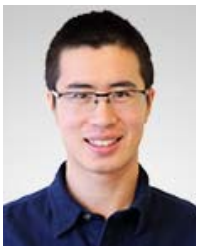

Zhenyun Qian (Member, IEEE) received the B.S. degree in electronic science and engineering from Southeast University, Nanjing, China, in 2011, and the M.S. and Ph.D. degrees in electrical and computer engineering from Northeastern University, Boston, MA, USA, in 2013 and 2017, respectively.

He worked as a Post-Doctoral Researcher with Northeastern University in 2017 and 2018, where he is currently a Research Assistant Professor with the Electrical and Computer Engineering Department. His research interests include piezoelectric MEMS resonators, 2D materials enhanced NEMS devices, zero-power environmental sensors, and agriculture sensor systems. He has published more than 60 articles and holds several device patents/applications in the field of MEMS/NEMS. He was a recipient of the Outstanding Paper Award at the 18th International Conference on Solid-State Sensors, Actuators, and Microsystems (Transducers 2015), the Best Paper Award at the 2017 European Frequency and Time Forum and International Frequency Control Symposium (IFCS-EFTF 2017), the Chinese Government Award for Outstanding Self-Financed Students Abroad in 2017, and the DARPA Riser 2018.

Matteo Rinaldi (Senior Member, IEEE) received the Ph.D. degree in electrical and systems engineering from the University of Pennsylvania in December 2010.

He worked as a Post-Doctoral Researcher with the University of Pennsylvania in 2011. He joined as an Assistant Professor with the Electrical and Computer Engineering Department, Northeastern University, in January 2012. His group has been actively working on experimental research topics and practical applications to ultra-low power MEMS/NEMS sensors (infrared, magnetic, chemical, and biological), plasmonic micro and nano electromechanical devices, medical micro systems and implantable micro devices for intra-body networks, reconfigurable radio frequency devices and systems, phase change material switches, and 2D material enabled micro and nano mechanical devices. He is currently a Full Professor with the Electrical and Computer Engineering Department, Northeastern University, and the Director of the Northeastern SMART a University Research Center that, by fostering partnership between university, industry, and government stakeholders, aims to conceive and pilot disruptive technological innovation in devices and systems capable of addressing fundamental technology gaps in several fields, including the Internet of Things (IoT), 5G, quantum engineering, digital agriculture, robotics, and healthcare. The research in his group is supported by several Federal grants (including DARPA, ARPA-E, NSF, and DHS), the Bill and Melinda Gates Foundation and the Keck Foundation with funding of $16+M since 2012. He is also the Founder and the CEO of Zepsor Technologies, a start-up company that aims to bring to market zero standby power sensors for various Internet of Things applications including distributed wireless fire monitoring systems, batteryless infrared sensor tags for occupancy sensing, and distributed wireless monitoring systems of plant health parameters for digital agriculture. He is also the owner of Smart MicroTech Consulting LLC, a company that routinely provides consulting services to government agencies, large companies and startups in the broad areas of micro and nano technologies, Internet of Things, wireless communication devices and systems, radio frequency devices and systems, and sensors. He has coauthored more than 150 publications in the aforementioned research areas and also holds 11 patents and more than ten device patent applications in the field of MEMS/NEMS.

Dr. Rinaldi was the recipient of the IEEE Sensors Council Early Career Award in 2015, the NSF CAREER Award in 2014, and the DARPA Young Faculty Award class of 2012. He received the Best Student Paper Award at the 2009, 2011, 2015 (with his student), and 2017 (with his student) IEEE International Frequency Control Symposiums, the Outstanding Paper Award at the 18th International Conference on Solid-State Sensors, Actuators and Microsystems, Transducers 2015 (with his student), and the Outstanding Paper Award at the 32nd IEEE International Conference on Micro Electro Mechanical Systems, MEMS 2019 (with his student).